

Scaling behaviour of charged hadron p_T distributions in pp and $p\bar{p}$ collisions

W. C. Zhang¹ and C. B. Yang²

¹School of Physics and Information Technology, Shaanxi Normal University, Xi'an 710119, People's Republic of China

²Institute of Particle Physics & Key Laboratory of Quark and Lepton Physics (MOE), Central China Normal University, Wuhan 430079, People's Republic of China

E-mail: ¹wenchao.zhang@snnu.edu.cn, ²cbyang@mail.ccnu.edu.cn

Abstract.

We report on a scaling behaviour in the transverse momentum (p_T) distributions for charged hadrons produced in proton-proton (pp) collisions with different center of mass energies ($\sqrt{s} = 0.9, 2.76$ and 7 TeV) at the Compact Muon Solenoid (CMS) detector. This scaling behaviour appears when the p_T is replaced by p_T/K , where K is a parameter and depends on \sqrt{s} . A similar scaling behaviour is observed in the p_T distributions of charged hadrons produced in proton-antiproton ($p\bar{p}$) collisions with $\sqrt{s} = 0.63, 1.8$ and 1.96 TeV at the Collider Detector at Fermilab (CDF). The particle production mechanism behind the scaling behaviour in the pp or $p\bar{p}$ collisions could be explained by the model of percolation of strings.

PACS numbers: 13.85.Ni, 13.87.Fh

Submitted to: *J. Phys. G: Nucl. Part. Phys.*

1. Introduction

One of the main goals in high energy collisions is to investigate the dynamics for particle productions. Several approaches are utilized to search for regularities in the particle production, one of them being the search for a scaling behaviour of some quantities versus suitable variables.

The scaling behaviour was first introduced in electron-nucleon deep inelastic scatterings (DIS) in which the structure functions depend not on the energy of DIS but on the ratio of the energy to the momentum transfer in the scattering [1, 2, 3]. In recent years, scaling behaviours were observed in nucleus-nucleus collisions. Ref. [4] showed that a scaling behaviour is exhibited in the pion p_T spectra with different collision centralities at midrapidity in Au+Au collisions at the Relativistic Heavy Ion Collider (RHIC). This scaling behaviour of pions was also found in noncentral regions in Au+Au and d+Au collisions [5]. An analogous scaling behaviour was observed in the proton and anti-proton p_T spectra with different collision centralities at midrapidity in Au+Au collisions at RHIC [6].

Recently, a universal scaling behaviour was presented in the p_T distributions of charged hadrons in pp collisions with $\sqrt{s} = 0.9, 2.36$ and 7 TeV at CMS [7]. This scaling behaviour is seen when the p_T distributions are expressed in a suitable variable, p'_T . p'_T at energy $\sqrt{s'}$ is defined in terms of p_T at energy \sqrt{s} and it is written as $p'_T = p_T(\sqrt{s'}/\sqrt{s})^{\frac{\lambda}{\lambda+2}}$, where λ is a parameter and it depends on p_T at energy \sqrt{s} . In this paper, we propose another method to search for the scaling behaviour of the charged hadron p_T distributions in pp collisions with $\sqrt{s} = 0.9, 2.76$ and 7 TeV. This scaling behaviour shows up when the p_T distributions are presented in another suitable variable, $z = p_T/K$. Here K is a free parameter which only depends on \sqrt{s} , rather than p_T at energy \sqrt{s} . Similar scaling behaviour is also searched for in the charged hadron p_T distributions in $p\bar{p}$ collisions with $\sqrt{s} = 0.63, 1.8$ and 1.96 TeV at CDF.

This paper is organized as follows. In section 2, the procedure to search for the scaling behaviour in pp and $p\bar{p}$ collisions is illustrated. Section 3 describes the scaling behaviour of charged hadrons in pp and $p\bar{p}$ collisions with different center of mass energies. Section 4 shows the comparison between the scaling behaviours presented in the variables z and p'_T . Finally in section 5, the possible particle production mechanism behind the scaling behaviour is discussed.

2. Method to search for the scaling behaviour

The method to search for the scaling behaviour of charged hadron p_T spectra at different energies in pp and $p\bar{p}$ collisions is similar to the one which was described in Refs. [4, 5, 6]. Here we will describe it briefly. When presented in a suitable variable $z = p_T/K$, the scaled p_T spectra at different center of mass energies in pp or $p\bar{p}$ collisions, $\Phi(z) = A \cdot (2\pi p_T)^{-1} d^2N/dp_T dy|_{p_T=Kz}$, will exhibit a universal scaling behaviour. Here the parameters A and K depend on the energy in the pp or $p\bar{p}$ collisions. While in

Refs. [4, 5, 6], parameters A and K depend on the centrality of the Au+Au or d+Au collisions. As a convention, K and A are set to be 1 for the highest energy collisions. Obviously, with different choices of A and K for the highest energy collisions, we get different scaling functions $\Phi(z)$. The arbitrariness of $\Phi(z)$ will disappear if the p_T spectra at different energies are presented in another variable, $u = z/\langle z \rangle = p_T/\langle p_T \rangle$. Here $\langle z \rangle = \int_0^\infty z\Phi(z)zdz / \int_0^\infty \Phi(z)zdz$. The normalized scaling distribution as a function of u is thus defined as $\Psi(u) = \langle z \rangle^2 \Phi(\langle z \rangle u) / \int_0^\infty \Phi(z)zdz$.

3. Scaling behaviour in pp and $p\bar{p}$ collisions

The charged hadron p_T spectra in pp ($p\bar{p}$) collisions with $\sqrt{s} = 0.9, 2.76$ and 7 (0.63, 1.8 and 1.96) TeV at CMS (CDF) were published in Refs. [8, 9, 10, 11]. The p_T distributions in CMS (CDF) data cover a range up to 200 (50) GeV/c, which is much larger than the p_T coverage of the data presented in Refs. [4, 5, 6]. Since A and K are both set to be 1 for the highest energy collisions, the scaling function $\Phi(z)$ for the pp collisions is nothing but the charged hadron p_T spectrum at $\sqrt{s} = 7$ TeV. As described in Ref. [12], the p_T spectrum of charged hadrons produced in high energy collisions follows a non-extensive statistical distribution, namely the Tsallis distribution [13, 14, 15]. Thus the scaling function for the pp collisions can be written as follows:

$$\Phi(z) = C_q \left[1 - (1 - q) \frac{z}{z_0} \right]^{\frac{1}{1-q}}, \quad (1)$$

where C_q , q and z_0 are free parameters, and $1 - q$ is a measure of the non-extensivity. These parameters are obtained by fitting the p_T spectrum at $\sqrt{s} = 7$ TeV with the Tsallis distribution in Eq. (1) using the least χ^2 s method, and they are tabulated in the second column of table 1. The χ^2 s divided by the number of degrees of freedom (*dof*), named reduced χ^2 s, for this fit is 3.7. The scaling parameters A and K for the pp collisions with $\sqrt{s} = 0.9$ and 2.76 TeV are determined by fitting the scaled Tsallis distribution,

$$\frac{1}{A} \Phi(p_T/K) = \frac{C_q}{A} \left[1 - (1 - q) \frac{p_T/K}{z_0} \right]^{\frac{1}{1-q}}, \quad (2)$$

to the p_T spectra at these two lower collision energies using the least χ^2 s method. Here only A and K are free parameters, C_q , q and z_0 are fixed to the values obtained at $\sqrt{s} = 7$ TeV. Table 2 presents A and K for the pp collisions with $\sqrt{s} = 0.9, 2.76$ and 7 TeV. The fits performed on the p_T spectra with $\sqrt{s} = 0.9$ and 2.76 TeV are worse than the fit on the p_T spectrum with $\sqrt{s} = 7$ TeV, which could be seen from the comparison among the reduced χ^2 s for these three fits.

Figure 1 shows the scaling behaviour of the charged hadron p_T spectra presented in z for the pp collisions at $\sqrt{s} = 0.9, 2.76$ and 7 TeV. In order to see how well the CMS data agree with the fitted curve, we define a ratio, $R = \text{experimental data}/\text{fitted results}$. The inset of figure 1 shows R as a function of z for all data points in the pp collisions with different energies. Except for a few data points which lie in the moderate p_T region with

$2 < z < 7$ GeV/c, all the data points have R values in the range 0.5-1.5, which implies that the scaling behaviour is true within an accuracy of 50%. Considering the fact that the data in the pp collisions cover about 15 orders of magnitude, the fits performed on the p_T spectra with $\sqrt{s} = 0.9, 2.76$ and 7 TeV are good.

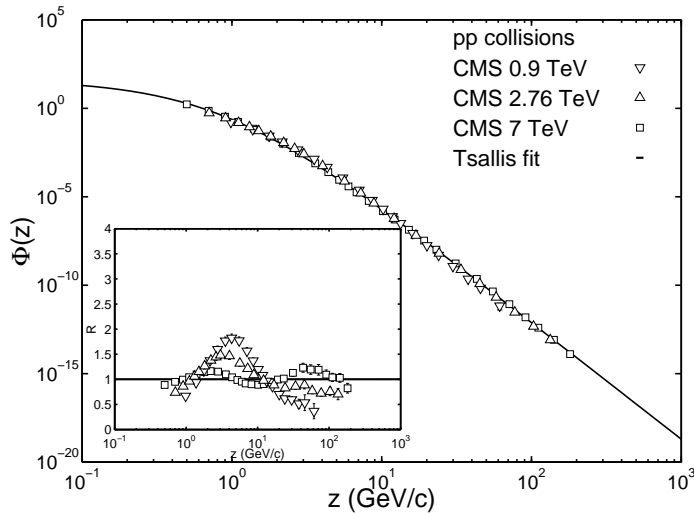


Figure 1. Scaling behaviour of the charged hadron p_T spectra presented in z for the pp collisions at $\sqrt{s} = 0.9, 2.76$ and 7 TeV. The solid curve is described by Eq. (1) with parameters tabulated in second column of table 1. The data points are taken from [8, 9]. The inset shows the distribution of the ratio between the experimental data and fitted results.

Table 1. The parameters C_q , q and z_0 for the scaling functions $\Phi(z)$ in the pp and $p\bar{p}$ collisions. The uncertainties quoted are statistical. The last line shows the reduced χ^2 s for the fit performed on the p_T spectrum with $\sqrt{s} = 7$ (1.96) TeV in the pp ($p\bar{p}$) collisions.

	pp collisions	$p\bar{p}$ collisions
C_q	40.9 ± 5.1	1066.4 ± 10.2
q	1.151 ± 0.001	1.123 ± 0.001
z_0 (GeV/c)	0.128 ± 0.004	0.154 ± 0.001
χ^2/dof	3.7	1.2

Table 2. Scaling parameters A and K for pp collisions with $\sqrt{s} = 0.9, 2.76$ and 7 TeV. The uncertainties quoted are statistical. The last column shows the reduced χ^2 s for fitting Eq. (2) to the p_T spectra at $\sqrt{s} = 0.9$ and 2.76 TeV.

\sqrt{s} (TeV)	K	A	χ^2/dof
0.9	0.51 ± 0.05	0.15 ± 0.07	52.3
2.76	0.74 ± 0.03	0.43 ± 0.11	19.7
7	1	1	-

For the $p\bar{p}$ collisions, the parameters C_q , q and z_0 are determined by fitting the Tsallis distribution in Eq. (1) to the p_T spectrum at $\sqrt{s} = 1.96$ TeV. These parameters are listed in the third column of table 1. The scaling parameters A and K for the $p\bar{p}$ collisions with $\sqrt{s} = 0.63, 1.8$ and 1.96 TeV are obtained in a similar way as those in the pp collisions and they are presented in table 3.

Figure 2 shows the scaling behaviour of the charged hadron p_T spectra presented in z for the $p\bar{p}$ collisions at $\sqrt{s} = 0.63, 1.8$ and 1.96 TeV. The R distribution as a function of z for the $p\bar{p}$ collisions is presented in the inset of this figure. In the low p_T region with $z < 10$ GeV/c, the data points and the fitted curve agree within 50%. In the high p_T region with $z > 10$ GeV/c, there is a large deviation between the data points and the fitted curve.

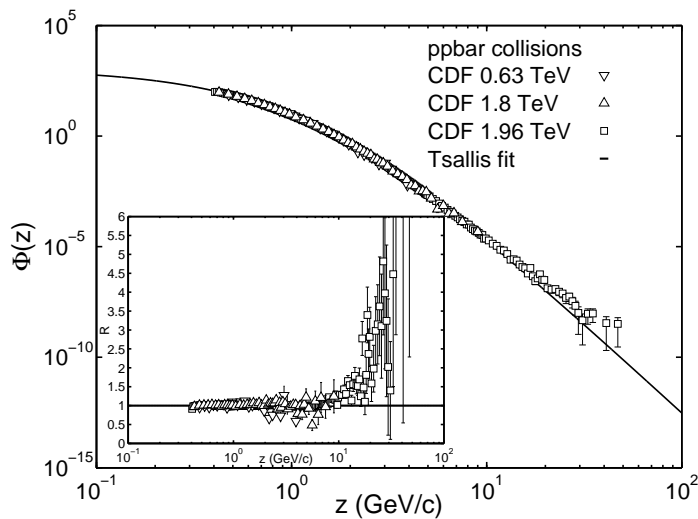


Figure 2. Scaling behaviour of the charged hadron p_T spectra presented in z for the $p\bar{p}$ collisions at $\sqrt{s} = 0.63, 1.8$ and 1.96 TeV. The solid curve is described by Eq. (1) with parameters tabulated in the third column of table 1. The data points are taken from [10, 11]. The inset is the distribution of the ratio between the experimental data and fitted results.

Table 3. Scaling parameters A and K for $p\bar{p}$ collisions with $\sqrt{s} = 0.63, 1.8$ and 1.96 TeV. The uncertainties quoted are statistical. The last column shows the reduced χ^2 s for the fits performed on the p_T spectra at $\sqrt{s} = 0.63$ and 1.8 TeV.

\sqrt{s} (TeV)	K	A	χ^2/dof
0.63	0.89 ± 0.02	2.85 ± 0.18	2.0
1.8	0.999 ± 0.004	2.28 ± 0.03	2.7
1.96	1	1	-

So far we have seen that the charged hadron p_T distributions in the pp and $p\bar{p}$ collisions indeed exhibit a scaling behaviour. However, the scaling function in Eq.

(1) relies on the choice of parameters A and K for the highest energy collisions. In order to eliminate this dependence on the choice, the scaling variable z is replaced by $u = z/\langle z \rangle$. In the pp ($p\bar{p}$) collisions, $\langle z \rangle$ for the charged hadrons is determined as 0.47 ± 0.02 (0.486 ± 0.002) GeV/c with the definite integral of z over the interval $[0, 200]$ ($[0, 50]$) GeV/c, which roughly corresponds to the p_T range measured by CMS (CDF). Plugging $\langle z \rangle$ as well as $\Phi(z)$ into $\Psi(u)$ defined in section 2, one can easily get the normalized scaling functions $\Psi(u)$ (see figure 3) for the pp and $p\bar{p}$ collisions as follows:

$$\Psi(u) = C'_q \left[1 - (1 - q') \frac{u}{u_0} \right]^{\frac{1}{1-q'}}. \quad (3)$$

Here the parameters C'_q , q' and u_0 in the pp ($p\bar{p}$) collisions are determined from C_q , q and z_0 at $\sqrt{s} = 7$ (1.96) TeV using the following expressions: $C'_q = \langle z \rangle^2 C_q / \int_0^\infty \Phi(z) z dz$, $q' = q$ and $u_0 = z_0 / \langle z \rangle$. Table 4 tabulates C'_q , q' and u_0 for $\Psi(u)$ in the pp and $p\bar{p}$ collisions.

Table 4. The parameters C'_q , q' and u_0 for the normalized scaling functions $\Psi(u)$ in the pp and $p\bar{p}$ collisions. The uncertainties quoted are due to the errors of parameters C_q , q and z_0 at $\sqrt{s} = 7$ and 1.96 TeV.

	pp collisions	$p\bar{p}$ collisions
C'_q	7.9 ± 1.2	6.63 ± 0.07
q'	1.151 ± 0.001	1.123 ± 0.001
u_0	0.27 ± 0.01	0.316 ± 0.001

The scaling behaviour of the p_T spectra for charged hadrons produced in the pp and $p\bar{p}$ collisions could be validated experimentally in the following way. With the normalized scaling functions in Eq. (3), we can calculate the ratio between the moments of the momentum distributions,

$$\frac{\langle p_T^n \rangle}{\langle p_T \rangle^n} = \int_0^\infty u^n \Psi(u) u du, \quad (4)$$

where $n = 2, 3, 4, \dots$. The integration interval for $\Psi_{pp}(u)$ ($\Psi_{p\bar{p}}(u)$), which corresponds to the range of $p_T / \langle p_T \rangle$ measured by CMS (CDF), is from 0 to 400 (100). Table 5 tabulates $\langle p_T^n \rangle / \langle p_T \rangle^n$ with $n = 2, 3, 4$ for the charged hadrons produced in the pp and $p\bar{p}$ collisions. Judging from Eq. (4), $\langle p_T^n \rangle / \langle p_T \rangle^n$ does only depend on the form of the normalized scaling function $\Psi(u)$ in the pp or $p\bar{p}$ collisions. If the scaling behaviour of the charged hadron p_T spectra exists, then the ratio between the moments of momentum should be a constant for collisions with different energies. As an example, the ratios between the moments of momentum with $n = 2$ are calculated using a combination of the measured data points at $\sqrt{s} = 0.9, 2.76$ and 7 TeV and the low and high p_T contributions determined from the fits of the Tsallis distribution in Eq. (1) to the p_T spectra at these energies. After a detailed calculation, the values of $\langle p_T^2 \rangle / \langle p_T \rangle^2$ for the pp collisions with $\sqrt{s} = 0.9, 2.76$ and 7 TeV are $1.9 \pm 0.1, 2.0 \pm 0.3$ and 2.1 ± 0.2 . Here the uncertainties quoted are due to the errors on the data points as well as the contributions

in the high and low p_T regions. These values and the value calculated with the integral of the normalized scaling function $\Psi(u)$ in the pp collisions, 2.1 ± 0.3 , are deemed to be consistent within uncertainties. This agreement confirms that the scaling behaviour of the charged hadron p_T spectra in the pp collisions at the CMS energies is true. We can also test the scaling behaviour of the charged hadron p_T spectra in the $p\bar{p}$ collisions at the CDF energies in a similar way.

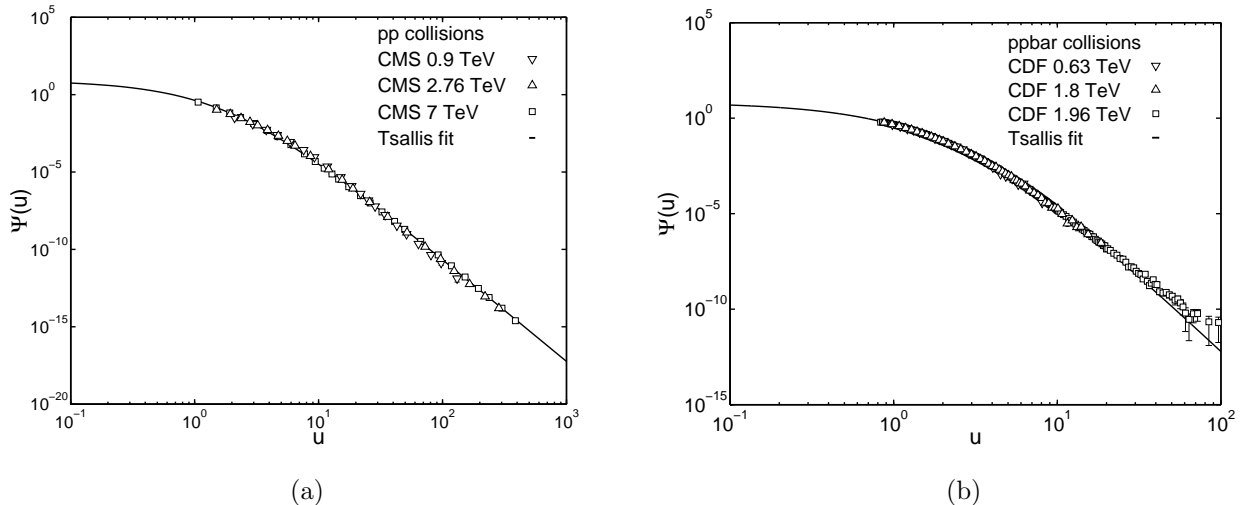


Figure 3. (a) ((b)), normalized scaling distribution as a function of variable u for the charged hadrons produced in the pp ($p\bar{p}$) collisions. The solid curves are described by Eq. (3). The CMS (CDF) data points are taken from [8, 9] ([10, 11]).

Table 5. $\langle p_T^n \rangle / \langle p_T \rangle^n$ calculated with Eq. (4) for the charged hadrons produced in the pp and $p\bar{p}$ collisions. The uncertainties quoted are due to the errors of parameters C'_q , q' and u_0 .

n	pp collisions	$p\bar{p}$ collisions
2	2.1 ± 0.3	1.86 ± 0.03
3	9.3 ± 1.4	6.1 ± 0.1
4	121.4 ± 20.7	36.4 ± 1.0

Now one would like to ask for the difference between the scaling functions in the pp and $p\bar{p}$ collisions. Figure 4 shows the comparison between the two normalized scaling functions $\Psi(u)$ for the pp and $p\bar{p}$ collisions. When u is small, the discrepancy between these two scaling functions is not so obvious in logarithm scale. In order to present it clearly, we define a variable $r = \Psi_{p\bar{p}}(u) / \Psi_{pp}(u)$ and show its distribution as a function of u in the inset of Fig. 4. When u is large, r decreases with the increase of u monotonically. This is confirmed by the comparison between the values of $\langle p_T^n \rangle / \langle p_T \rangle^n$ in the pp and $p\bar{p}$ collisions (see table 5). Because of small difference between these two normalized scaling functions at small u , the value of $\langle p_T^n \rangle / \langle p_T \rangle^n$ in the pp collisions is close to that

value in the $p\bar{p}$ collisions for small n . However, for large n , the value of $\langle p_T^n \rangle / \langle p_T \rangle^n$ in the pp collisions differs significantly from the value in the $p\bar{p}$ collisions due to the big difference between these two normalized scaling functions at large u .

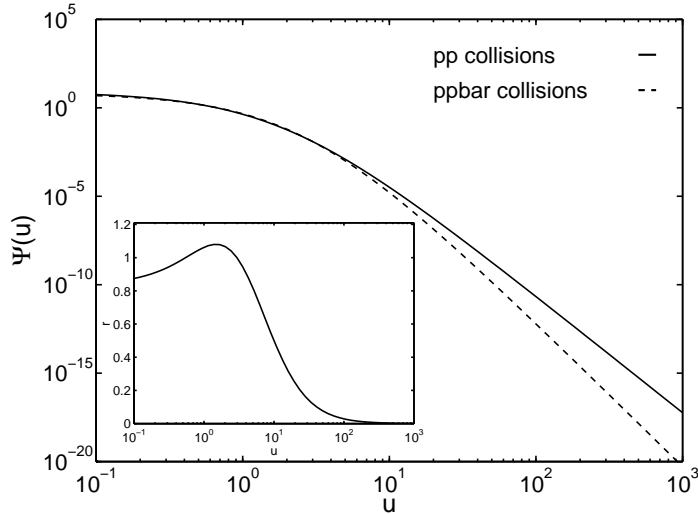


Figure 4. Comparison between the normalized scaling functions $\Psi(u)$ in the pp and $p\bar{p}$ collisions. The inset is the distribution of r as a function of u .

4. Comparison between the scaling behaviours presented in z and p'_T

As described in Ref. [7], there is a scaling behaviour when the charged hadron p_T spectra in the pp collisions at the CMS energies are presented in the variable p'_T . The p_T spectrum at \sqrt{s} is connected with the p'_T spectrum at $\sqrt{s'}$ via $p'_T = p_T(\sqrt{s'}/\sqrt{s})^{\frac{\lambda}{\lambda+2}}$, where $\lambda = 0.13 + 0.1(4p_T^2/10)^{0.35}$. Figure 5 shows the p_T distributions presented in p'_T in the pp collisions with $\sqrt{s} = 0.9, 2.76$ and 7 TeV. In this figure, the p_T spectra at $\sqrt{s} = 2.76$ and 0.9 TeV have been rescaled to the p'_T spectrum at $\sqrt{s'} = 7$ TeV. The latter spectrum is described by the Tsallis fit in Eq. (1) with parameters in the second column of table 1. The inset of figure 5 shows the distribution of the ratio between the experimental data and fitted results. When p'_T is smaller than 20 GeV/c, the scaling behaviour of the charged hadron p_T spectra presented in p'_T is true within an accuracy of 50%. This accuracy is comparable to the accuracy of the scaling behaviour of the charged hadron p_T spectra presented in z . However, when p'_T is greater than 20 GeV/c, the p_T spectra at $\sqrt{s} = 2.76$ and 0.9 TeV start to deviate significantly from the p_T spectrum at $\sqrt{s} = 7$ TeV.

5. Discussions

We have shown that there is a scaling behaviour in the p_T distributions of charged hadrons produced in the pp ($p\bar{p}$) collisions at the CMS (CDF) energies. This scaling behaviour is observed when a linear transformation is applied on p_T . The Tsallis

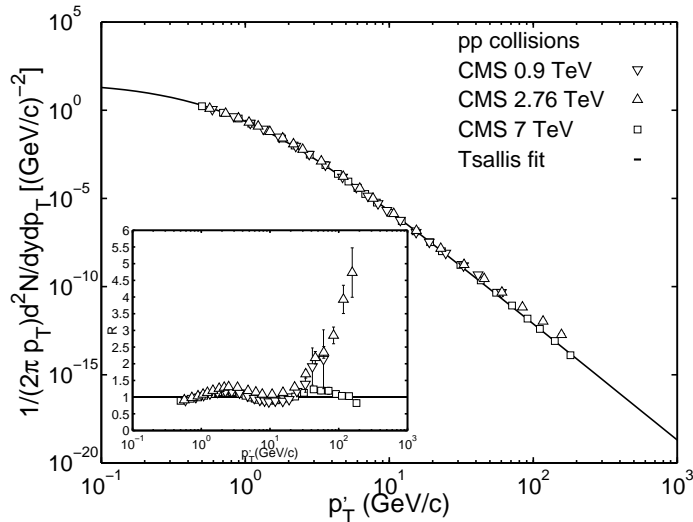


Figure 5. Scaling behaviour of the charged hadron p_T spectra presented in p'_T in the pp collisions with $\sqrt{s} = 0.9, 2.76$ and 7 TeV. The solid curve is described by Eq. (1) with parameters in the second column of table 1. The data points are taken from [8, 9]. The inset shows the distribution of the ratio between the experimental data and fitted results.

distribution can be applied to describe the universal shape of the spectra behind this scaling behaviour. In order to understand the particle production mechanism behind this scaling behaviour, the model of percolation of strings is utilized [16]. In this model, color strings are stretched between the two colliding hadrons in the pp or $p\bar{p}$ collisions. These strings will split into new strings with the emission of $q\bar{q}$ pairs. Observed hadrons are formed through this quark pair emission. The transverse area of a color string is $S_1 = \pi r_0^2$, where $r_0 = 0.2$ fm. If there are n strings, they may overlap with each other and thus form a cluster with a transverse area of S_n . The p_T distribution at energy $\sqrt{s'}$ could be related to the p_T distribution at energy \sqrt{s} by a linear transformation on p_T at energy $\sqrt{s'}$: $p_T \rightarrow p_T / ((nS_1/S_n) \sqrt{s'} / (nS_1/S_n) \sqrt{s})^{1/4}$. Here nS_1/S_n gives the degree of string overlap. If strings just get in touch with each other, then $S_n = nS_1$ and $nS_1/S_n = 1$. If strings maximumly overlap with each other, then $S_n = S_1$ and $nS_1/S_n = n$ with $n > 1$. Comparing the p_T transformation in this model with the one used in the way to search for the scaling behaviour, $p_T \rightarrow p_T/K$, we know that K gives the ratio between the degrees of string overlap for the collisions at $\sqrt{s'}$ and \sqrt{s} . For the pp ($p\bar{p}$) collisions at CMS (CDF), \sqrt{s} is set to be 7 (1.96) TeV and $\sqrt{s'}$ is set to be $0.9, 2.76$ and 7 ($0.63, 1.8$ and 1.96) TeV. As described in Ref. [16], the degree of string overlap, nS_1/S_n , grows with the increase of the energy. Thus K should also grow with the increase of the energy. That's indeed what we observed in tables 2 and 3. We found that in the pp ($p\bar{p}$) collisions the degrees of string overlap at $\sqrt{s'} = 0.9$ and 2.76 (0.63 and 1.8) TeV are $(6.8 \pm 2.7)\%$ and $(30.0 \pm 4.9)\%$ ($(62.7 \pm 5.6)\%$ and $(99.6 \pm 1.6)\%$) of the degree of string overlap at $\sqrt{s} = 7$ (1.96) TeV. As a summary, the scaling behaviour we observed in the p_T distributions of charged hadrons produced at different colliding

energies can be phenomenologically understood within the string percolation model.

Acknowledgments

This work was supported by Shaanxi Normal University. This work was also supported in part by the National Natural Science Foundation of China under Grant Nos. 11075061 and 11221504, by the Ministry of Education of China under Grant No.306022, and by the Programme of Introducing Talents of Discipline to Universities under Grant No. B08033.

References

- [1] Bjorken J D and Paschos E A 1969 *Phys. Rev.* **185** 1975
- [2] Feynman R P 1969 *Phys. Rev. Lett.* **23** 1415
- [3] Koba Z, Nielsen H B, and Olesen P 1972 *Nucl. Phys. B* **40** 317
- [4] Hwa R C and Yang C B 2003 *Phys. Rev. Lett.* **90** 212301
- [5] Zhu L L and Yang C B 2007 *Phys. Rev. C* **75** 044904
- [6] Zhang W C, Zeng Y, Nie W X, Zhu L L and Yang C B 2007 *Phys. Rev. C* **76** 044910
- [7] Praszalowicz M 2011 *Phys. Rev. Lett.* **106** 142002
- [8] Khachatryan V *et al* (CMS Collaboration) 2011 *J. High Energy Phys.* **08** 086
- [9] Khachatryan V *et al* (CMS Collaboration) 2012 *Eur. Phys. J. C* **72** 1945
- [10] Abe F *et al* (CDF Collaboration) 1988 *Phys. Rev. Lett.* **61** 1819
- [11] Aaltonen T *et al* (CDF Collaboration) 2009 *Phys. Rev. D* **79** 112005
- [12] Rybczynski M, Wlodarczyk Z and Wilk G 2012 *J. Phys. G: Nucl. Part. Phys.* **39** 095004
- [13] Tsallis C 1988 *Stat. Phys.* **52** 479
- [14] Tsallis C 2009 *Eur. Phys. J. A* **48** 161
- [15] Tsallis C 2009 *Introduction to Nonextensive Statistical Mechanics* (Berlin: Springer)
- [16] Braun M A, Moral F del and Pajares C 2002 *Phys. Rev. C* **65** 024907